APPLICATION OF CT FILTER ALGORITHMS TO DIGITIZED FILM DATA

James A. Morman

Reactor Analysis and Safety Division
Argonne National Laboratory
9700 S. Cass Avenue
Argonne, IL 60439

INTRODUCTION

The CT studies performed thus far in the RAS division have been based on neutron radiographs of two 7-pin reactor fuel bundles which were subjected to over-power accident simulations in the TREAT reactor. The tests as referenced below were named LO5 and LO6. As a result of the tests, the pins were severely damaged, with molten fuel and steel spreading throughout the fuel assembly. After removal of parts of the test vehicle, the remaining assembly is approximately 2-m long, and about 10-cm diameter.

Radiography and Digitization

The neutron radiographs are produced at the NRAD reactor facility at ANL-West in Idaho. The beam port used for the radiography is shaped to a rectangular opening of 43.2 by 25.4 cm. The standard foil cassette is approximately this same size, and a near-parallel-beam geometry is achieved with only a 1.5% magnification factor.

The fuel pin bundle is suspended on a precision rotation mechanism between the reactor and the neutron detector so that it can be rotated for the multiple angles needed for the CT process. The detector consists of a packet of two foils: one 0.05-cm thick cadmium foil to attenuate thermal neutrons, and one indium foil to capture the epithermal (1.45 eV) neutrons. After an irradiation time of 30 - 60 minutes, the indium foil is removed and placed in contact with a sheet of photographic film (normally type T). After the decaying indium exposes the film, it is processed and prepared for digitization.

Digitization is performed on a Perkin-Elmer scanning micro-densitometer with a resolution of 12 bits (1 part in 4096) corresponding to an optical density range of 0 to 5. Normally, only densities up to about 3.2 are used. The current set of optics allows an aperture as small as 25 microns in either x or y direction. Because of their large size, the standard radiographs are scanned in two parts, each half being 23.5 by 21.6 cm, with a 1.5-cm overlap. Scribed lines and a step wedge allow for alignment of the two halves into one 42-cm long image.

Reconstruction Technique

The RAS reconstruction codes are based on the filtered back-projection technique, using standard fast Fourier transforms and filter algorithms. Because of the length of the fuel assemblies, and the fact that they are held only at the top by the rotation mechanism, it is nearly impossible to achieve a perfect vertical alignment, so a major part of the analysis time is spent in rotating and aligning the images. As part of this computerized alignment, each image is also normalized to a constant exposure time, based on the data in a neutron absorbing step wedge that is imaged along with the fuel pins. All computer codes were loosely developed from those given in the Donner Algorithms prepared for the National Cancer Institute [1] and are currently run on a PDP-11/60 computer.

LO5/LO6 Parameters

For each of the fuel bundles, radiographs were made at 2.4 degree rotations through 180 degrees, for a total of 76 views. For LO5, the aperture of the densitometer was set to 200 (horizontal) by 400 (vertical) microns. Each scan row consisted of 1176 pixels with 541 rows per image in order to scan just over one half of the 43-cm long radiograph. The final reconstructions were square arrays of 291 x 291 (200 μ) for LO5, and 707 x 707 (50 μ) for LO6.

Table I summarizes the parameters used for the digitization and reconstruction of images from the two tests. Because of the slight magnification, the actual spatial resolution is slightly (98.5 %) smaller than the aperture size. Each reconstruction used only the data from one y-elevation on the radiograph, so the "thickness" of each CT slice is 400 μ. While the reconstruction technique is mostly standard, the selection of the appropriate filter is the most time consuming part of the process, simply because of the speed of the computer now in use. The filter ultimately determines how well the reconstruction represents reality.

FILTER SELECTION

When the filtering is done in frequency space, the filters become multipliers on the terms of the discrete transform. This means that filters can be changed easily for comparisons. Figure 1 shows a typical frequency spectrum from a rotated radiograph before and after filtering,

Table I. Parameters for Tests LO5 and LO6.

	LO5	LO6
Scan aperture, x (μ)	200	50
Scan aperture, y (μ)	400	400
Points per scan row		
entire radiograph	1176	3049
cropped image	291	707
Reconstructions		
δx, δy (μ)	200	50
δz (μ)	400	400
Filter parameters		
order (2n)	3	3
frequency maximum	0.1	0.015
Computer time per reconstruction (min)	44	168

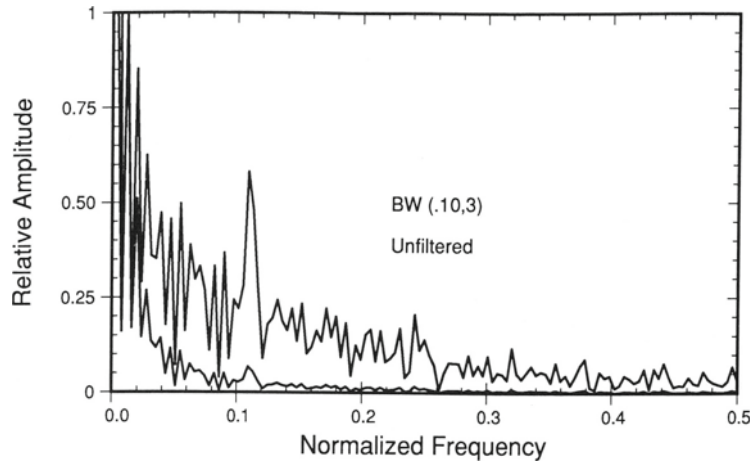

Fig. 1. Typical Fourier Spectral Density Before and After Filtering.

with the spectra renormalized to highlight differences. The filter is meant to reduce slowly varying components such as non-uniform background, reduce the noise caused by statistical fluctuations in the data, yet enhance the details. The elimination of the low frequencies is hard to see from the plots, but the normalized data do show the reduction of the higher frequency contributions. Most of the data is grouped in the low frequency region.

The three filters that we have been using are termed the Hann, Hamming, and Butterworth, and their functional forms are:

$$F(f) = 0.5|f| + 0.5|f| \cos \frac{\pi f}{f_m} \tag{1}$$

$$F(f) = 0.5|f| + 0.46|f| \cos \frac{\pi f}{f_m} \tag{2}$$

$$F(f) = \frac{f}{[1 + (f/f_m)^{2n}]^{1/2}} \quad . \tag{3}$$

In the above equations, f_m is a rollover frequency and 2n is the order.

These filters were chosen as starting points because they were implemented in the Donner algorithms. Initial reconstructions with the Hann and Hamming were not particularly good, and it was found that the results using these two filters could be reproduced by adjusting the parameters of the Butterworth filter, Eq. (3).

The Butterworth is the most flexible, with terms to control the width and cross-over frequency. Figure 2 shows the shape of the Butterworth filter for several combinations of f_m and n. While the differences in the filtered frequency spectra as shown in Fig. 1 appear minimal, the effect on the actual reconstructions can be seen in the next set of figures.

As noted above, the two experiments were performed with 7-pin fuel bundles. In order to provide a reference when viewing the reconstructions, Fig. 3 shows the cross section of the as-built fuel assembly. The fuel pins were stainless-steel-clad, and composed of

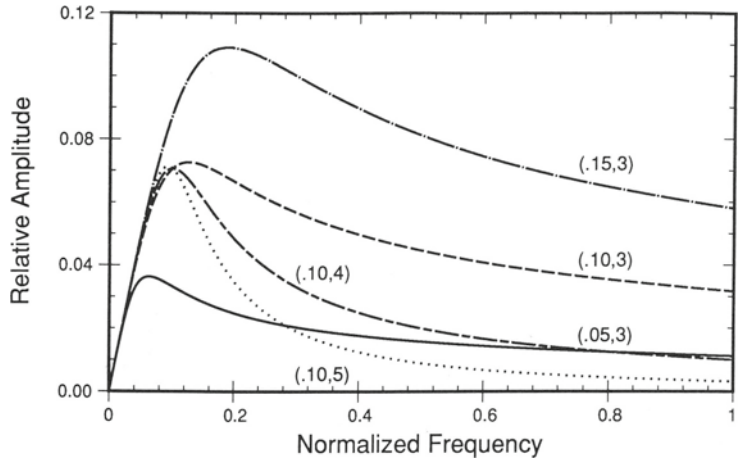

Fig. 2. Butterworth Filter Shapes in Normalized Frequency Space.

annular pellets with an OD of 5.0 mm and central hole of 1.9 mm. The clad has a thickness of 0.4 mm. The tri-fluted flow tube has an OD of 2.6 cm and a thickness of 0.09 cm.

LO5 FILTER COMPARISONS

Figure 4 shows an LO5 reconstruction near the bottom of the fuel pins, where little damage has been done. Note the grain patterns and lack of distinguishing features. The thick steel outer tube shows significant scattering in the data values. Figures 5 and 6 show the effect of moving the rollover frequency lower into the frequency spectrum. As more of the lower frequencies are included, less noise is seen in the thick steel section, but the pin shapes become hexagonal.

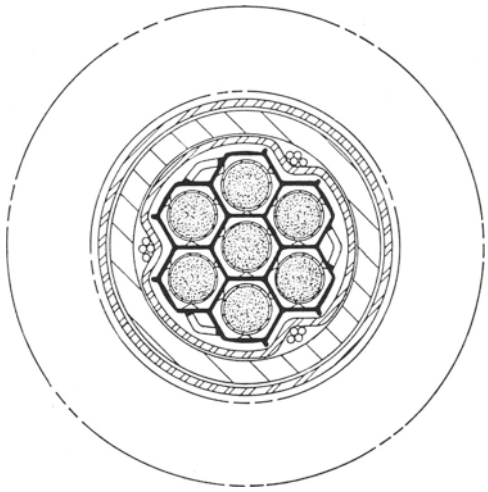

Fig. 3. Cross Section of the 7-Pin Fuel Assemblies Used for Tests LO5 and LO6.

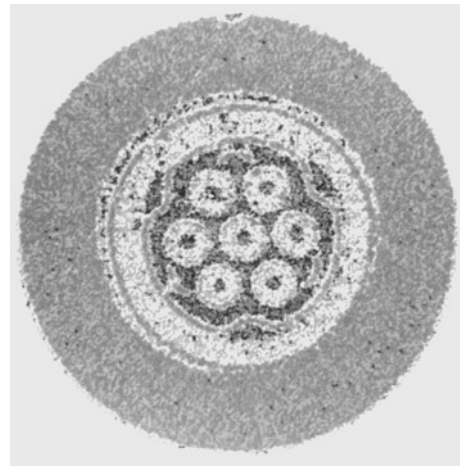

Fig. 4. Reconstruction of LO5 Data with Parameters f_m=0.25, 2n=3.

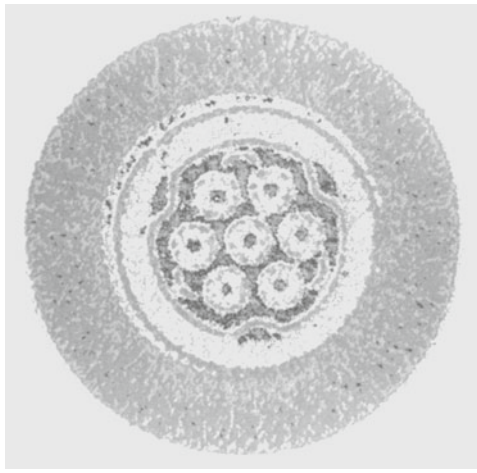

Fig. 5. Reconstruction of L05 Data with Parameters f_m=0.15, 2n=3.

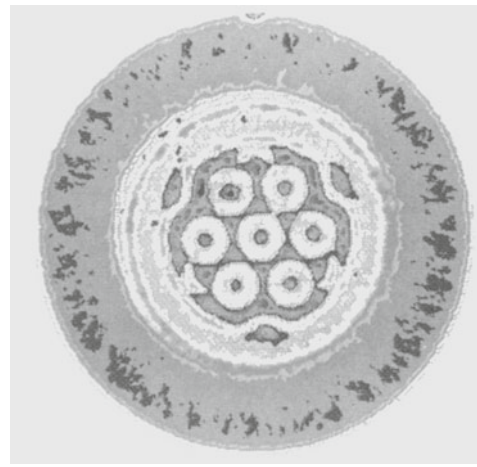

Fig. 6. Reconstruction of L05 Data with Parameters f_m=0.05, 2n=3.

Another way to see the effect of the filter is to look at the histograms of these reconstructions, which represent the number of pixels within an image that have the same density value. The set of histograms in Fig. 7 corresponds to the reconstructions of Figs. 4-6. They show that when more of the low frequencies are included, the valleys between the peaks are lower, so the peaks which represent different materials are better defined. As less of the low frequencies and more of the high are included, peak definition worsens and the limits of material densities become questionable. However, the inclusion of too much of the low frequency part of the spectrum produces artifacts, such as the hexagonal shaped pins of Fig. 6.

L06 FILTER COMPARISONS

For the L06 test, the aperture of the densitometer was reduced to see if better definition of the clad or grid spacers could be obtained. Two problems occurred which have reduced the quality of the initial

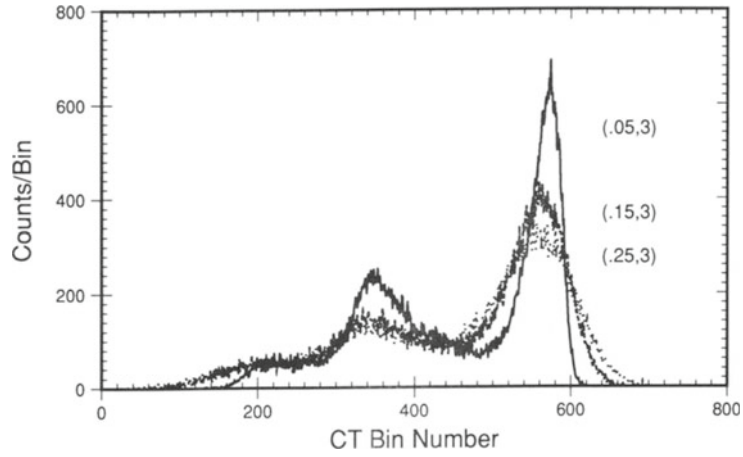

Fig. 7. Histograms from the L05 Reconstructions of Figs. 4-6.

Fig. 8. Reconstruction of LO6 Data with Parameters f_m=0.015, 2n=1.

reconstructions from LO6. First, the section of the radiographs that have been digitized so far is at an elevation where the pins were more severely disrupted than those in LO5. Within this region, no intact pins can be found and the assembly is a very dense mixture of fuel and steel. Figure 8 shows this mixture, with perhaps a hint of separate areas in the debris. The filter used here was a Butterworth of order 1 and f_m=0.015.

The second problem occurred when the radiographs were digitized. Because of the unusually high densities, standard densitometer settings caused some of the data values to be outside of the useable limits. As a result the high densities containing most of the information have been cut off. Even with these problems, some filter tests were done. Figures 9 and 10 show the same elevation with filter orders of 2.0 and 2.5. While some difference is apparent, little detail can be seen in any of the reconstructions. Adjustments have been made for scanning the remaining parts of the radiographs and it is expected that the results will improve considerably.

Fig. 9. Reconstruction of LO6 Data with Parameters fm=0.015, 2n=2.

Fig. 10. Reconstruction of LO6 Data with Parameters fm=0.015, 2n=2.5.

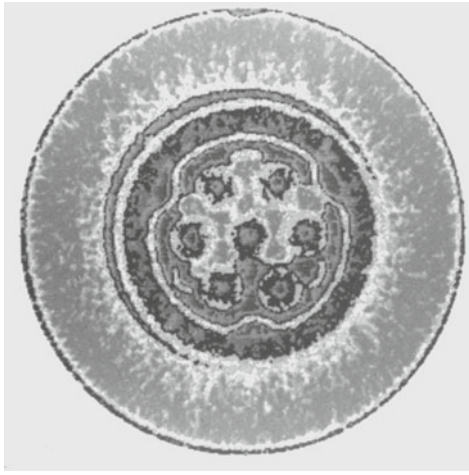

Fig. 11. Reconstruction of LO5 Data with Parameters f_m=0.1, 2n=3, z=-55 mm.

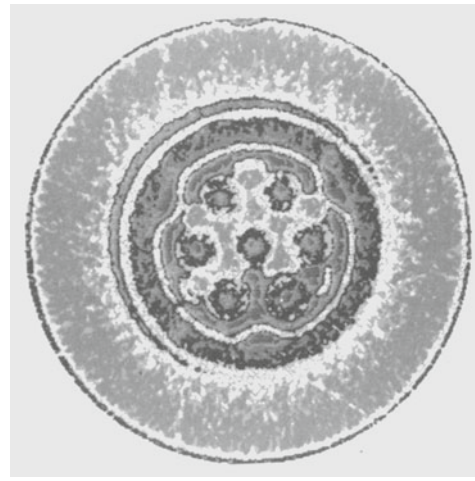

Fig. 12. Reconstruction of LO5 Data with Parameters f_m=0.1, 2n=3, z=-53 mm.

SUMMARY

As a summary of results, Figures 11-14 show LO5 reconstructions using a Butterworth filter of order 3 and rollover frequency of 0.1 that are axially separated by 2 mm. In Fig. 11, the edges of the fuel pellets and perhaps the clad are clearly visible, along with the central hole in the pellets and some restructuring that has occurred in the fuel. Figures 12-14 show the accumulation of a slug of molten debris around nearly intact fuel pins. Comparison of this region with metallography data showed excellent agreement, and the CT technique offers an option to the sectioning, polishing and examination of the fuel pins.

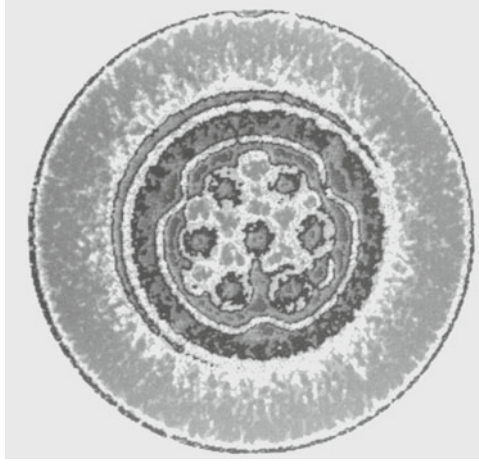

Fig. 13. Reconstruction of LO5 Data with Parameters f_m=0.1, 2n=3, z=-51 mm.

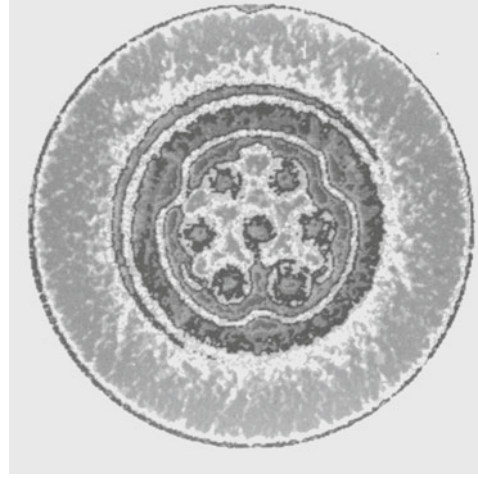

Fig. 14. Reconstruction of LO5 Data with Parameters f_m=0.1, 2n=3, z=-49 mm.

While reasonable results have been obtained for the LO5 data using the Butterworth filter, filter testing is one of the main areas needing further research. Advanced, higher order filters promise better results, and the selection of better filters for application to high-resolution radiograph data is currently being studied.

REFERENCES

1. R. H. Huesman, G. T. Gullberg, W. L. Greenberg and T. F. Budinger, "RECLBL Library Users Manual: Donner Algorithms for Reconstruction Tomography," Lawrence Berkeley Laboratory Pub. 214 (Oct., 1977).